



# Invalidity of continuum theories of electrolytes in nanopores

B. Corry<sup>a</sup>, S. Kuyucak<sup>b</sup>, S.H. Chung<sup>a,\*</sup>

<sup>a</sup> *Protein Dynamics Unit, Department of Chemistry, Australian National University, Canberra, ACT 0200, Australia*

<sup>b</sup> *Department of Theoretical Physics, Research School of Physical Sciences, Australian National University, Canberra, ACT 0200, Australia*

Received 8 February 2000

## Abstract

Continuum theories of electrolytes are widely used to describe physical processes in various biological systems, even when the system dimensions are comparable to the Debye length. We test the validity of the mean field approximation in Poisson–Boltzmann and Poisson–Nernst–Planck theories by contrasting their predictions with those of Brownian dynamics simulations in cylindrical pores of varying radius. We find that both continuum theories largely overestimate shielding effects when the pore radius is smaller than two Debye lengths, and, therefore, they cannot be used to describe the physics of electrolytes in nanopores. © 2000 Published by Elsevier Science B.V. All rights reserved.

## 1. Introduction

During the last few decades, continuum theories of electrolytes have found a new niche in the description of physical processes that take place in the salty waters of cells [1–4]. Many of these applications involve membranes, proteins and other macromolecules – systems whose dimensions are much larger than the Debye length of ions so that the validity of the underlying mean field approximation does not come into question. There is also a growing field of applications of continuum theories in ion channels – nanopores formed by proteins across biological membranes that provide pathways for ion flow [5]. For example, the Poisson–Boltzmann (PB)

equation is used to calculate the potential energy profile of ions in equilibrium situations (e.g. Refs. [6–9], and references therein), while the Poisson–Nernst–Planck (PNP) equations are employed to calculate ion flux across membrane channels (e.g. Refs. [10–13], and references therein). Considering that complete screening of an ion's charge occurs at about 4 Debye lengths in a bulk solution, and at physiological concentrations (0.15 M) the Debye length is 8 Å, it is not clear how these continuum theories could be applied to narrow cylindrical pores whose diameters are less than 1 or 2 Debye lengths. So far there have been no systematic studies of the continuum theories to check their validity in nanopores, and in the face of the rapid growth of their applications in ion channels, it seems imperative that such a study should be carried out as a matter of urgency. Here, we test the validity of the mean field approximation in PB and PNP theories by comparing their predictions for various physical

\* Corresponding author. Fax: +61-2-6247-2792; e-mail: shin-ho.chung@anu.edu.au

quantities with those obtained from Brownian dynamics (BD) simulations in otherwise identical situations. BD is suitable for this purpose because the motion of all the ions in a given system are traced individually according to the Langevin equation. Hence, a long-time average of physical quantities should accurately reflect the actual physical behaviour of the system.

## 2. Continuum theories and Brownian dynamics

The PB theory provides a classical electrostatic description of a system in which fixed external and boundary charges, represented by a density  $\rho_{\text{ex}}$ , are surrounded by mobile ions in a dielectric medium. The main assumption of the theory is that at equilibrium, the distribution of the mobile ions in the system can be approximated by a continuous number density given by the Boltzmann factor

$$n_\nu = n_{\nu 0} \exp(-z_\nu e\phi/kT), \quad (1)$$

where  $n_{\nu 0}$  is the bulk (or reference) number density of ions of species  $\nu$ ,  $z_\nu e$  is their charge and  $\phi$  is the potential. Upon feeding this density into Poisson's equation

$$\epsilon_0 \nabla \cdot (\epsilon \nabla \phi) = - \sum_\nu z_\nu e n_\nu - \rho_{\text{ex}}, \quad (2)$$

one obtains the PB equation

$$\epsilon_0 \nabla \cdot (\epsilon \nabla \phi) = - \sum_\nu z_\nu e n_{\nu 0} \exp(-z_\nu e\phi/kT) - \rho_{\text{ex}}. \quad (3)$$

For a given boundary, Eq. (3) is solved numerically using a standard finite difference algorithm [2,3], which yields the potential and concentration profiles of ions everywhere in the system. In the following, we use concentration of ions  $c_\nu$  instead of  $n_\nu$ , which are related by  $n_\nu$  (SI units) =  $10^3 N_A c_\nu$  (mol/l).

A corresponding continuum description of flux  $\mathbf{J}_\nu$  due to an ion species  $\nu$  is provided by the Nernst–Planck equation, which combines the diffusion due to a concentration gradient with that from a potential gradient

$$\mathbf{J}_\nu = -D_\nu \left( \nabla n_\nu + \frac{z_\nu e n_\nu}{kT} \nabla \phi \right), \quad (4)$$

where  $D_\nu$  is the diffusion coefficient of ion species  $\nu$ . The potential  $\phi$  in Eq. (4) is determined from the solution of Poisson's Eq. (2). The PNP Eqs. (2) and (4) are solved simultaneously using a finite difference algorithm similar to the PB case [12], yielding the potential, concentration and flux of ions in the system.

In continuum theories, ion concentration and flux are described by continuous quantities that represent the macroscopic, space–time averages of microscopic motion of individual ions. Whether this assumption is still valid when the system size is comparable to the Debye length can be tested directly by performing BD simulations in identical systems, and computing the ion concentration and flux from the time-average of ionic motions. In BD, the trajectory of each ion in the system is followed using the Langevin equation

$$m_i \frac{d\mathbf{v}_i}{dt} = -m_i \gamma_i \mathbf{v}_i + \mathbf{F}_R + z_i e \mathbf{E}_i + \mathbf{F}_S, \quad (5)$$

where  $m_i$ ,  $z_i e$  and  $\mathbf{v}_i$  are the mass, charge and velocity of the  $i$ th ion. In Eq. (5), the effect of the water molecules is represented by an average frictional force with a friction coefficient  $m_i \gamma_i = kT/D_i$ , and a stochastic force  $\mathbf{F}_R$  arising from random collisions. The fourth term in Eq. (5) is the total electric force acting on the ion due to other ions, fixed and induced surface charges in the boundary, and the applied electric field. It is computed by solving Poisson's Eq. (2) using the usual boundary conditions, that is,  $\mathbf{E}_1 \times \hat{\mathbf{n}} = \mathbf{E}_2 \times \hat{\mathbf{n}}$  and  $\epsilon_1 \mathbf{E}_1 \cdot \hat{\mathbf{n}} = \epsilon_2 \mathbf{E}_2 \cdot \hat{\mathbf{n}}$ , where the indices 1 and 2 refer to inside and outside the boundary. The iterative numerical method employed for this purpose is detailed elsewhere [14,15]. Rather than solving Poisson's equation at each time step, which would be computationally prohibitive, a system of lookup tables is used [16]. The electric field and potential due to one- and two-ion configurations are precalculated at a number of grid points and stored in a set of tables. During simulations, the potential and field at desired points are reconstructed by interpolating between the table entries and using the superposition principle. The last term in Eq. (5) describes the short-range part of the ion–ion potential using the standard  $[(R_1 + R_2)/r_{12}]^9$  form, which emulates the hard-sphere collisions

in the primitive model quite well. The radius of the colliding ions are taken as  $R_{\text{Na}} = 0.95$  and  $R_{\text{Cl}} = 1.81$  Å. The ions are elastically scattered from the channel and reservoir boundaries when they come into contact with them. The Langevin Eq. (5) is solved at discrete time steps ( $\Delta t = 100$  fs) following the algorithm in Ref. [17]. For further technical details of BD simulations, we refer to Refs. [16,18,19]. Throughout, bulk values of the diffusion coefficients are employed in all theories, i.e.  $D_{\text{Na}} = 1.33 \times 10^{-9}$  and  $D_{\text{Cl}} = 2.03 \times 10^{-9}$  m<sup>2</sup>/s.

### 3. Tests of continuum theories

We have performed a number of control studies to ensure that the results obtained from the solution of PB and PNP equations are in agreement with those obtained from the BD simulations under bulk conditions. Details of these studies will be published in a longer article. Here we report the results of tests of continuum theories in nanopores with dimensions typical of ion channels – the total length of the cylindrical pore is 35 Å and its radius is varied from  $r = 3$  to 13 Å (see the top of Fig. 1). The corners of the cylinder are rounded with a radius of curvature 5 Å to avoid difficulties in numerical solutions of Poisson's equation with sharp corners. Reservoirs with a radius of 30 Å and are attached on either side of the pore. The height of the reservoirs is 25 Å for a  $r = 3$  Å pore, which is progressively reduced for larger radii to keep the volume fixed. The dielectric constant is  $\epsilon = 80$  inside the boundary (water) and  $\epsilon = 2$  outside, which is representative of proteins forming ion channels. A NaCl solution with an average concentration of 0.3 M is used in the comparisons, represented by a total of 24 Na<sup>+</sup> and 24 Cl<sup>-</sup> ions in BD simulations. The reason for using this higher value instead of the more typical 0.15 M is entirely statistical; twice as many ions leads to a better accuracy in BD simulations. The results, once expressed in terms of the Debye length, are more or less independent of the concentration used. We note that the Debye lengths are 7.9 and 5.6 Å, respectively, for 0.15 and 0.3 M solutions.

#### 3.1. PB theory versus BD

Dynamic behaviour of an ion inside or near the vicinity of a channel is determined by the total force

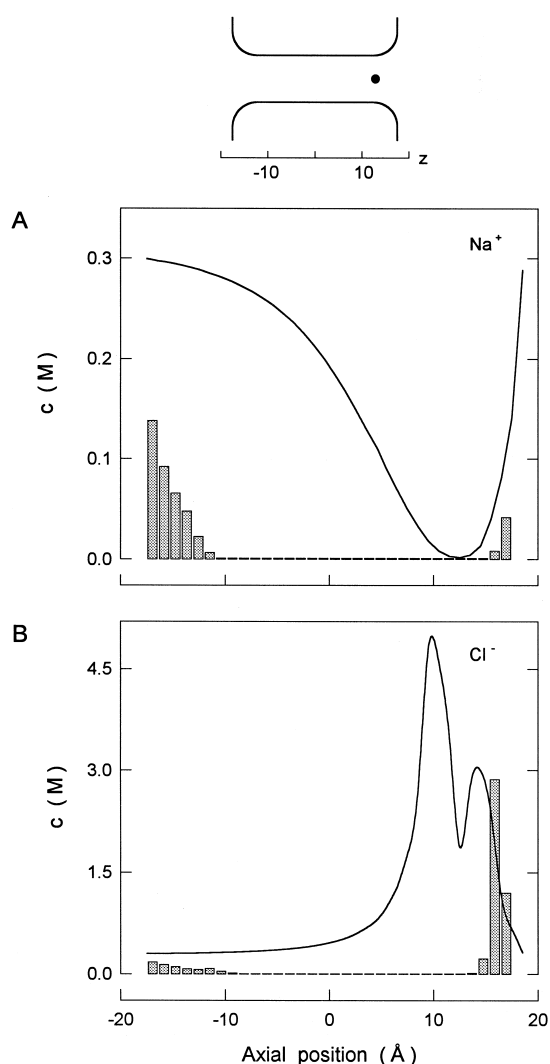


Fig. 1. Test of the PB theory for an electrolyte in a  $r = 3$  Å pore. (A) Average concentrations of cations (A) and anions (B) along the channel when there is a test ion (Na<sup>+</sup>) at  $z = 12.5$  Å. In BD, the channel is divided into 32 layers and the average concentration value in each layer is represented by the histograms. The corresponding PB values are indicated by the solid lines.

acting on it. In the absence of mobile ions, the repulsive force on an ion from the dielectric boundary leads to a large potential barrier that is high enough (7 kT for  $r = 3$  Å) to prevent the ion from entering the pore. In the presence of an ionic atmosphere, the counter charges around the ion are expected to provide some shielding of the repulsive

force and thereby reduce the potential barrier. The PB theory is known to allow a large amount of shielding for an ion even in narrow pores [6]. The aim of this study is to test, through comparisons with the more realistic BD simulations, whether this effect is genuine or a chimera arising from the breakdown of the mean field approximation in systems with sizes smaller than the Debye length.

The two critical quantities to be tested are the amount of screening charge around a test ion and the resulting force on it compared to that of a single ion ( $c = 0$ ). In Fig. 1 we compare the concentration profiles for cations (A) and anions (B) in a  $r = 3 \text{ \AA}$  pore when there is a test ion ( $\text{Na}^+$ ) at  $z = 12.5 \text{ \AA}$ . The sodium and chloride concentrations obtained from the PB calculations exhibit a behaviour similar to that of a bulk situation – there is a net screening charge near the test ion and within a few Debye lengths both concentration profiles relax to the reservoir value of 0.3 M. The BD simulations, on the other hand, provide an entirely different picture. Ions can only access the mouth region of the pore, and the interior remains completely devoid of both types of ions. To give a quantitative indication of this difference, we note that the total screening charge in the pore (difference of negative and positive charges) is  $-0.61e$  in PB and  $-0.01e$  in BD. This huge disparity in screening charges leads to very different results on the force acting on the test ion as shown in Fig. 2. The PB results predict nearly an order of magnitude suppression of the force compared to that of single ion ( $c = 0$ ). In contrast, the BD results follow closely the force on a single ion near the mouth region (no shielding) and deviate from it somewhat in the interior pointing to some shielding effect, though it is nowhere near the PB level. In BD, this shielding in the channel interior arises because an anion gets trapped in the channel forming a dipole with the test cation. This is a failure of our short range ion–ion potential, which though suitable for purposes of comparison with the PB theory, actually simulates a weak electrolyte. That is, there is a relatively deep minimum in the Na–Cl pair potential at contact that favours the binding of the two ions. This problem is resolved when the hydration forces are taken into account by deriving the ion–pair potentials from the potential of mean force calculations in molecular dynamics simulations

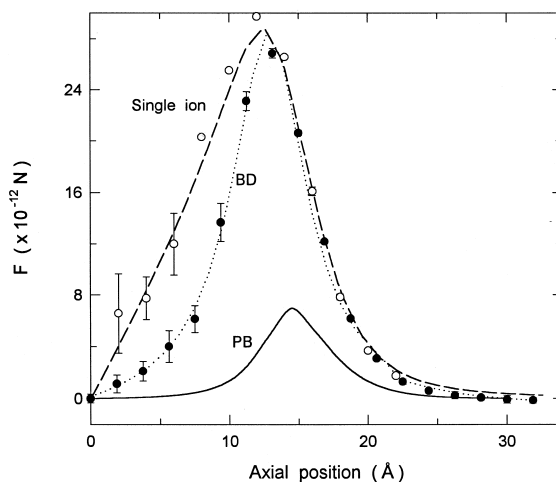


Fig. 2. Force acting on a test ion ( $\text{Na}^+$ ) as it is moved along the axis of  $r = 3 \text{ \AA}$  pore. The PB results are shown by the solid line and BD by the filled circles fitted with a dotted line. The force acting on a single ion ( $c = 0$ ) is indicated by the dashed line for reference. The open circles are the results of BD simulations employing realistic ion–ion potentials derived from molecular dynamics calculations. Each BD point represents the average of a 160 ns simulation period.

[20,21]. When such a realistic ion–ion potential is employed in BD simulations, the anomalous looking behaviour disappears, and the force tracks the single ion results everywhere as indicated by the open circles in Fig. 2.

Having established the failure of the PB approach in narrow channels, we next explore its domain of validity, that is, how large the pore radius has to be to get an agreement between the PB and BD results. For this purpose, we study in Fig. 3 the changes in the screening charge in the pore (A) and the force on the test ion at  $z = 12.5 \text{ \AA}$  (B) as the pore radius is increased. The total screening charge in PB remains nearly constant with the increasing radius, the slight increase being due to approaching bulk conditions (note that the screening charge in the channel is less than  $-e$  because the channel volume is limited to  $z = \pm 17.5 \text{ \AA}$ ). In BD, this charge is nearly zero at  $r = 3 \text{ \AA}$  but it steadily rises with  $r$ , converging to the PB value at about  $r = 11 \text{ \AA}$  or 2 Debye lengths. A similar result follows for the force on the ion in Fig. 3B. The force in BD initially coincides with that of a single ion at  $r = 3 \text{ \AA}$ , and with increasing radius, it gradually converges to the PB values at around

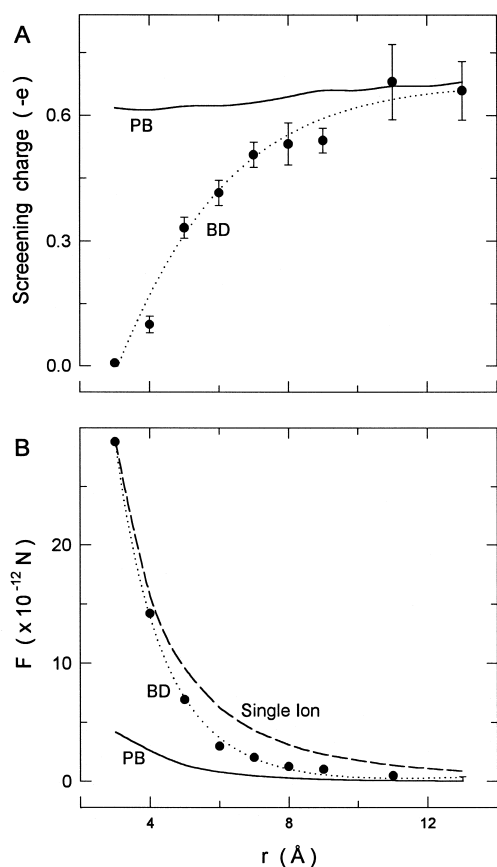


Fig. 3. (A) The net screening charge in the channel, when a cation is held at  $z = 12.5 \text{ \AA}$ , is plotted as a function of the pore radius. The PB results are shown by the solid line and the BD values by the filled circles fitted with the dotted line. (B) Force on the same cation as the pore radius is increased. The PB (solid line), BD (filled circles fitted with a dotted line) and single ion results (dashed line) are indicated in the figure. Each BD point represents the average of a 150 ns simulation period.

2 Debye lengths. This study clearly shows that biological ion channels, whose radii are typically less than  $5 \text{ \AA}$ , are outside the domain of the validity of the PB theory.

### 3.2. PNP theory versus BD

The failure of PB theory in nanopores is a direct consequence of its continuum assumptions that leads to large shielding effects, which are not observed in

realistic simulations. Since the PNP theory is based on the same continuum assumptions, similar discrepancies are expected to arise in concentration and flux calculations in PNP when compared to the BD simulations. In Fig. 4 we compare the sodium concentration profiles obtained from PNP equations with those constructed from BD simulations in a  $r = 3 \text{ \AA}$  pore with reservoirs as discussed above. (The chloride concentrations are not shown since they are very similar to the sodium results.) The average concentrations are held at 0.5 and 0.1 M in the left and right reservoirs, respectively, and a 105 mV potential difference is applied between the reservoir ends. Concentrations in BD are found by dividing the pore and reservoirs into layers, counting the number of ions in each layer at each time step and averaging over the entire simulation. In PNP the concentrations are calculated by averaging over all the grid points in each layer. Apart from entrance effects, the PNP results change almost linearly across the pore as would be expected in a bulk electrolyte. Since the sodium and chloride concentrations in the pore exhibit similar profiles, they more or less cancel each other providing an almost perfect shielding situation with practically no induced surface charges to hinder permeation of ions. In other words, the ion-channel

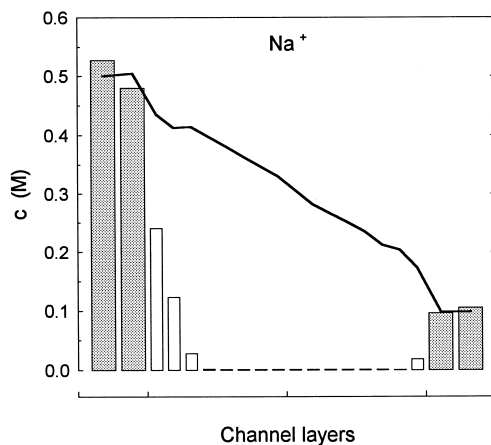


Fig. 4. Comparison of sodium concentration profiles in PNP with BD in a  $r = 3 \text{ \AA}$  pore in the presence of both a concentration and a potential gradient. The pore is divided into 16 layers and reservoirs into 2 layers. The average concentration values in layers are represented by the histograms in BD (reservoir values are shaded) and by the solid line in PNP.

interactions are completely ignored in PNP, allowing charge to be transported across the pore as if the dielectric boundary did not exist (i.e.  $\epsilon_{\text{protein}} = 80$ ). When the ions are treated individually as in BD simulations, an entirely different picture emerges (Fig. 4). The ion concentration drops exponentially as one moves into the pore and almost vanishes in the centre. This result is a consequence of the fact that ions enter the pore singly most of the time and meet a sharply rising potential barrier created by induced charges. Ions occasionally probe inside the pore, but the energy barrier combined with the Boltzmann distribution of ion energies, make this increasingly less probable, resulting in the exponential drop of concentration. Thus, when ions are treated with integrity there are no shielding effects inside narrow pores, and the representation of ions as continuous charge densities as in PNP leads to erroneous results. The differences between the concentrations found from PNP and BD diminish as the radius of the pore is increased, converging at  $r \approx 14 \text{ \AA}$ .

Since the potential and concentration are determined self consistently in PNP, the errors committed in concentrations are expected to affect the potential results and lead to inaccuracies in the ion flux through the pore. To illustrate the magnitude of these errors and their dependence on pore size, we plot in Fig. 5A the normalised conductances found from PNP and BD against the pore radius. In this study a symmetric solution of 0.3 M and an applied potential of 105 mV are used. The conductances have been normalised by the cross sectional area of the pore to factor out the trivial increase in conductance with area. The slight reduction in PNP results with increasing  $r$  is due to the access resistance varying as  $1/r$  as opposed to the  $1/r^2$  variation in the cylinder resistance [22]. The PNP conductances are actually very similar to those found without a dielectric boundary, confirming the fact that ions permeate the pore as if there are no ion-channel interactions. The BD simulations exhibit a dramatically different result: The conductance vanishes in a  $r = 3 \text{ \AA}$  pore and is suppressed by more than an order of magnitude in other narrow pores compared to the PNP results. Clearly the repulsive boundary forces successfully block ionic currents in these narrow pores as no shielding due to counter ions is possible. As the channel radius is increased further, the conduc-

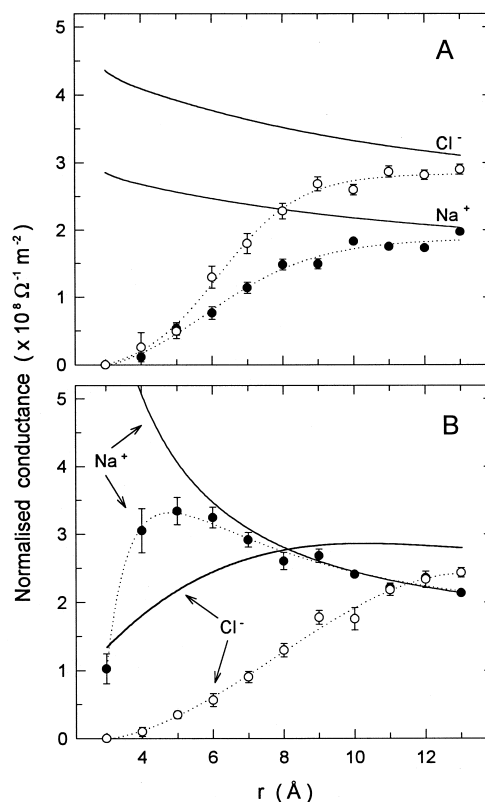


Fig. 5. Normalised conductance of  $\text{Na}^+$  and  $\text{Cl}^-$  ions in a pore without (A) and with (B) fixed charges are plotted against the pore radius. The BD results are indicated by circles which are fitted with a dotted lines, and the PNP results are shown by the solid lines. Each BD data point is obtained from a 3.6  $\mu\text{s}$  simulation period.

tance in BD rises, converging towards the PNP results at  $r \approx 13 \text{ \AA}$ .

Biological ion channels usually have excess charges in the protein walls, which allow oppositely charged ions to overcome the boundary forces and thus enable their permeation while prohibiting the counter ions from entering the channel. We examine the effect of such charges by placing a ring of eight monopoles each with a charge  $-0.09e$  at both ends of the channel in the pore walls ( $z = \pm 12.5 \text{ \AA}$ ). This arrangement of charges almost completely cancels the barrier seen by a  $\text{Na}^+$  ion entering a  $r = 4 \text{ \AA}$  pore, and similar charges have been used in applications of PNP [11]. In Fig. 5B, we show the nor-

malised conductance as in A except with the inclusion of the fixed charges. The presence of negative charges in the pore leads to an increase in cation current and a decrease in anion current in both theories as expected. However, the discrepancy between the PNP and BD results remains in narrow pores especially for the anion current. The fixed charges spoil the perfect shielding encountered in a bare pore and thereby lead to some improvement in the PNP results (e.g. faster convergence in sodium current), but there is still sufficient shielding left in PNP to lead to an order of magnitude larger chloride current compared to BD in pores with  $r < 6 \text{ \AA}$ .

#### 4. Conclusions

We have demonstrated unequivocally that nanopores with radii smaller than two Debye lengths are outside the domain of validity of the continuum theories of electrolytes, and therefore, they should not be used to describe the physics of ion channels. In fact, shielding effects are almost negligible in narrow channels, and therefore, use of Poisson's equation rather than PB is recommended for potential and force calculations in ion channels.

#### Acknowledgements

This work was supported by grants from the ARC and the NHMRC of Australia. The calculations were carried out with the Fujitsu VPP-300 and Linux Alpha Cluster of the ANU Supercomputer Facility.

#### References

- [1] T.F. Weiss, Cellular Biophysics, MIT Press, Cambridge, MA, 1996, Vols. 1, 2.
- [2] M.E. Davis, J.A. McCammon, Chem. Rev. 90 (1990) 509.
- [3] K.A. Sharp, B. Honig, Annu. Rev. Biophys. Biophys. Chem. 19 (1990) 301.
- [4] B. Honig, A. Nicholls, Science 268 (1995) 1144.
- [5] B. Hille, Ionic Channels of Excitable Membranes, 2nd edn., Sinauer Associates Inc., Sunderland, MA, 1992.
- [6] P.C. Jordan, R.J. Bacquet, J.A. McCammon, P. Tran, Biophys. J. 55 (1989) 1041.
- [7] P. Weetman, S. Goldman, C.G. Gray, J. Phys. Chem. 101 (1997) 6073.
- [8] C. Adcock, G.R. Smith, M.S.P. Sansom, Biophys. J. 75 (1998) 1211.
- [9] G.R. Dieckmann, J.D. Lear, Q. Zhong, M.L. Klein, W.F. DeGrado, K.A. Sharp, Biophys. J. 76 (1999) 618.
- [10] B. Eisenberg, Contemp. Phys. 39 (1998) 447.
- [11] D.P. Chen, L. Xu, A. Tripathy, G. Meissner, B. Eisenberg, Biophys. J. 76 (1999) 1346.
- [12] M.G. Kurnikova, R.D. Coalson, P. Graf, A. Nitzan, Biophys. J. 76 (1999) 642.
- [13] R.S. Eisenberg, J. Membr. Biol. 171 (1999) 1.
- [14] M. Hoyles, S. Kuyucak, S.H. Chung, Biophys. J. 70 (1996) 1628.
- [15] M. Hoyles, S. Kuyucak, S.H. Chung, Comput. Phys. Commun. 115 (1998) 45.
- [16] M. Hoyles, S. Kuyucak, S.H. Chung, Phys. Rev. E 58 (1998) 3654.
- [17] W.F. van Gunsteren, H.J.C. Berendsen, Mol. Phys. 45 (1982) 637.
- [18] S.C. Li, M. Hoyles, S. Kuyucak, S.H. Chung, Biophys. J. 74 (1998) 37.
- [19] S.H. Chung, M. Hoyles, T.W. Allen, S. Kuyucak, Biophys. J. 75 (1998) 793.
- [20] E. Guàrdia, R. Rey, J.A. Padró, Chem. Phys. 155 (1991) 187.
- [21] E. Guàrdia, R. Rey, J.A. Padró, J. Chem. Phys. 95 (1991) 2823.
- [22] J. Hall, J. Gen. Physiol. 66 (1975) 531.